Risk Assessment at Puerto Vallarta due to a Local Tsunami.

Elizabeth Trejo Gomez (e291058@gmail.com)
Universidad de Guadalajara https://orcid.org/0000-0002-6743-4888
Francisco Javier Núñez-Cornú
Universidad de Guadalajara - Centro Universitario de la Costa Puerto Vallarta

Research Article

Keywords: Tsunami hazard, Rivera Plate, Jalisco Block, Bahía de Banderas, Puerto Vallarta

Posted Date: April 28th, 2021

DOI: https://doi.org/10.21203/rs.3.rs-337768/v1

Risk assessment at Puerto Vallarta due to a local tsunami.

Elizabeth Trejo-Gómez[1] and Francisco Javier Núñez-Cornú[1]

[1] *C. A. Centro de Sismología y Volcanología de Occidente (CA-UdG-276 SisVOc), Centro Universitario de la Costa, Universidad de Guadalajara, Puerto Vallarta, México.*

Abstract

The Jalisco region in western Mexico is one of the most seismically active in the country. The city of Puerto Vallarta is located at Bahía de Banderas on the northern coast of Jalisco., Currently there exists a Seismic Gap in the Northern coast of Jalisco (Vallarta Gap). Historically seismogenic tsunamis have affected the coast of Jalisco. In this work, the risk due to a local tsunami in the city of Puerto Vallarta is a function of the interaction between hazard and vulnerability. We model the tsunami hazard, generation and propagation, using the initial conditions for a great earthquake (Mw ≥ 8.0) similar to those that occurred in 1787 at Oaxaca and in 1995 at Tenacatita Bay, Jalisco. Vulnerability is estimated with available data for the years 2010-2015 with sociodemographic variables and the location of **g**overnment, commercial or cultural facilities. The area with the highest vulnerability and risk is between the valleys of the Ameca and Pitillal Rivers, extending to a distance greater than 5.1 km from the coastline and affecting an area of 30.55 km2. This study does not consider the direct damage caused by the tsunamigenic earthquake and aftershocks; it assumes that critical buildings in the region, mostly hotels, would not collapse after the earthquake and could serve as a refuge for its users. The first (It) tsunami wave arrives to Puerto Vallarta (Cuale) 19 min after the earthquake with a height (Hi) of 3.7 m, the Run Up (At) arrives 74 min after earthquake with a height (Hr) of 5.6 m.

Keywords: Tsunami hazard, Rivera Plate, Jalisco Block, Bahía de Banderas, Puerto Vallarta.

1 Introduction

The Jalisco region, in western Mexico (Figure 1), is one of the most seismogenic regions in Mexico, with many past destructive earthquakes of great magnitude, some of which generated important tsunamis. The largest instrumentally-recorded historic earthquake in the 20th century in Mexico was an M = 8.2, on June 3, 1932, and located off the coast of Jalisco (Núñez-Cornú 2011). A few days later, on June 18, 1932, a magnitude M = 7.8 earthquake struck the region again. Sánchez and Farreras (1993) have proposed both earthquakes were tsunamigenic. Nevertheless, the most destructive tsunamigenic event in the region was a probable submarine slump landslide involving marine sediments provided by the Armería River accumulated on the continental shelf that took place on June 22, 1932. It was responsible for destroying a resort at Cuyutlán (Colima state), causing a maximum water layer height of 15 m and an estimated flooding extent of 1 km along 20 km of coast.

In 1995, an Mw = 8.0 earthquake occurred off the coast of Jalisco, caused a tsunami that affected a 200-km-long coastline with damage limited to low-lying coasts (Ortiz et al. 1995; Ortiz et al. 2000; Trejo et al. 2015). The 1995 earthquake ruptured only the southern half of the area proposed for the 1932 events (Singh et al. 1985), suggesting that the northern coast of Jalisco, including Bahía de Banderas (BdB) (Figure 1), presents a seismic gap (Vallarta Gap) that might rupture and generate a local tsunami.

The BdB region (Figure 1) could be affected by tele-, regional, and local tsunamis. To date, there is no historical report for significant damages caused by tele-tsunamis or regional tsunamis at BdB. In the case of tele-tsunamis, the waves reported historically are less than one meter; however, the hazard exists because of the possibility that bay resonance could amplify tsunami waves and generate a seiche that could cause much damage. Dressler and Núñez-Cornú (2007) calculated the bay's eigen-period (resonance period) at T = 2,726 s (45 min 30 sec) using a hydropneumatic method and a preliminary bathymetric model of the BdB. Specific sites such as Boca de Tomatlán, Marina Vallarta, Plaza Genovesa and, Playa de Los Muertos regions in Puerto Vallarta, were evaluated for an incoming wave to BdB of 10 cm amplitude and different arrival periods, and the results vary at the different sites with amplitudes higher than 100 cm and oscillations of different periods.

No important earthquake in the region was reported on March 12, 1883, even though a tsunami was reported in Las Peñas (currently Puerto Vallarta):

> "It was observed that the sea withdrew its ordinary beaches to a considerable extent and at a considerable distance from the coast, revealing some mountains and valleys in the background... It is not known with certainty what the ocean brought about in its withdrawal, but after some time, it reoccupied its box with enough noise and impulse" (Orozco and Berra 1888).

Four places in Puerto Vallarta were analyzed by Núñez-Cornú et al. (2006) for an $Mw = 8.0$ earthquake to estimate tsunami run-up height (Hr), and they concluded that a tsunami would enter at Pitillal river´s valley as a 2 m $\leq Hr \leq$ 4 m and in the area of the Ameca river's valley as a 5 m $\leq Hr \leq$ 7 m. The estimated run-up was imprecise in shallow waters (depth < 50 m), due to the resolution of the information used, because it does not discriminate between different beaches in Puerto Vallarta. For this scenario a specialized study is required to generate more datasets that characterize the shallow water marine relief in Puerto Vallarta because in these areas the tsunami´s wave is refracted, and hazards could be increased.

The coastal community at Puerto Vallarta faces the challenge of mitigating the tsunami hazard from local earthquakes. This fact requires developing accurate risk-reduction measures based on thorough tsunami hazard, vulnerability, and risk assessments. Núñez-Cornú and Carrero-Roa (2012) suggest that land managers with an adequate perception of risk could make decisions to prevent a disaster by reducing vulnerability through design actions based on scientific data and risk assessment theory. Risk assessment consists of three phases: evaluation, management, and perception. Reducing vulnerability requires mitigation actions such as sustainable land uses, possible civil works, and population preparation (knowing how to take shelter to stay safe, etc.). Civil Defense Authorities need to generate contingency response protocols, determine the recovery and reconstruction actions in the affected area, and evaluate economic losses in the community due to a false alert.

Perception is a critical phase of risk assessment, as decision-makers can create a disaster based on the misperception of hazard behavior. One such example is the catastrophy

caused by Hurricane Katrina in 2005 in New Orleans, USA(Dixon 2015) with more than 1800 fatalities. Katrina remains the costliest disaster in the U.S. history. Another example occurred as a result of the 1985 eruption of Nevado del Ruiz Volcano, Colombia, whereby a failure in communication lead to the destruction of the city of Armero by a lahar causing more than 24,000 fatalities (Mileti et al. 1991). Such a disaster occurs after a catastrophic chain of hazard and social events (Smith 2013). For Núñez-Cornú and Carrero-Roa (2012), it is not the lack of information or misperception of hazard that causes the disaster, rather a disaster results from the inadequate management of socially acceptable risk, based on three factors: (a) denying the hazard, (b) maintain the inertia of territory without planning, and (c) transfer the costs of risk to others.

An assessment of the tsunami risk for a coastal community is the primary initial information required for the design of social education programs, and the implementation of protocols by local emergency institutions and the civil defense both in public and private buildings (Hebenstrait et al. 2003). Currently, Puerto Vallarta has the highest population density on the Jalisco coast, and the second largest urban area in the state and plays an essential role in the regional economic development, mainly through tourism. The 2020 population census preliminary results counted 291,839 (Instituto de Información Estadística y Geográfica de Jalisco INEGI 2020). More than 90% of Puerto Vallarta inhabitants live in our study area (Figure 2), and there is an average floating population of approximately 50,000 people during the high tourist season, from October to April.

The objective of this work is to carry out a first evaluation of the Risk that a local seismogenic tsunami represents for the city of Puerto Vallarta. Hazard is modeled from potential tsunami inundation zones based on numerical simulations of a major thrust earthquake occurring in the Vallarta Gap. The vulnerability is obtained with data from public databases. This study does not consider direct damages caused by that earthquake; it assumes that critical buildings in the region, mostly hotels, would not collapse after the earthquake and could serve as a refuge for its users.

2 Tectonic Setting and local Tsunamis

In Western Mexico, three tectonic plates interact, the Rivera Plate (RP) and the Cocos Plate (CP), which are subducted along the Mesoamerican trench (MAT) under the North American Plate (NOAM). This process has produced deformation and fragmentation of the continental crust giving rise to a tectonic unit known as the Jalisco Block (JB) and several triple points have been proposed (Figure 1). The tectonics of this region are not clearly understood (Luhr et al. 1985; Bourgois et al. 1988; DeMets and Stein 1990; Allan et al. 1991; Garduño and Tibaldi 1991). The JB is defined to the north by the extensive structure known as the Tepic-Zacoalco fault zone (TZR), which continues east with the Chapala – Tula Rift Zone (CTR) and the Pacific coast, and continues south to the Pacific coast by Colima fault zone (CRZ). The CRZ is similar in structure and age to the TZR and is defined on land and offshore by recent seismic activity (Pacheco et al. 2003). The TZR consists of several tectonic depressions with extensional and right lateral movements, which also indicate deep crustal failures between the JB and NOAM (Núñez-Cornú et al. 2002). The western border of JB defined by the MAT.

Dañobeitia et al. (2016) and Núñez-Cornú et al. (2016) found that to the north of the Marias Islands, there is no clear evidence of an active subduction zone. Instead, faulting is observed to the west of the Marias Islands, while to the south between the María Magdalena and María Cleofas islands, the subducted slab of the Rivera Plate is delineated by regional seismicity. They also report the existence of a 100 km long tectonic structure south of Maria Cleofas Island, Sierra de Cleofas (SC). The SC is oriented N-S and marks the boundary between RP and JB, possibly as a result of compression of RP against JB. It establishes the beginning of the current subduction and associated seismic activity. Urías et al. (2016) propose that the existence of Ipala Canyon (IC) is related to extension produced by the abrupt change in RP convergence and that IC may be the southeast limit of a major forearm block (Figure 1), called Banderas Forearc Block (BFB).

The Jalisco region has experienced numerous destructive earthquakes of great magnitude with epicenters along the coast and inland. The historical macroseismic data for the region date back to 1544 (Núñez-Cornú 2011). Núñez - Cornú et al. (2018) reported that

at least 22 major earthquakes with M ≥ 7.0 took place in the past 474 years. Suter (2019) studied and concluded that the 1563, May 27, M_I = 8, earthquake took place offshore Puerto de Navidad (now named as Barra de Navidad), and the estimated rupture area to be similar to the 1932 and 1995 earthquakes. Suter (2018) analyzed the macroseismic data of the October 2, 1847, Jalisco Earthquake, and concluded that there were two earthquakes the same day. The first one, a subduction type earthquake, took place at 07:30 am offshore Tecomán, Colima with an estimated magnitude of Mw 7.4 (Figure 1); the second, a shallow intraplate type earthquake with an estimated magnitude M_I 5.7, took place at 09:30 am and affected the western part of the CTR, destroying the city of Ocotlán and other towns nearby. To date, thirteen big destructive earthquakes (Table 1, Figure 1) associated with the subduction process of RP below NOAM along the Jalisco coast region have been identified. Only for seven of these, are there local data of relevant damage caused by the tsunamis generated. It is necessary to add two tsunamis (1883 and 1932-06-22) probably generated by submarine landslides. However, no geological studies have been for Puerto Vallarta to identify damage and/or effects of historical tsunamis.

3 Methods

The study area is the city of Puerto Vallarta, Jalisco (Figure 2) located between 105° 20' W, 20° 43' N and 105° 11' W, 20° 32' N. In this study, we present an estimation of the risk in Puerto Vallarta due to the occurrence of a local tsunami after a great magnitude earthquake with an epicenter offshore along the northern part of the Middle America Trench. Risk is a function of hazard and vulnerability for a specific area; in this study, we consider the hazard is a result of the coastal flood generated by a local tsunami. Subsequently, mapping the population, housing, and vital facilities located in the hazard impact area is necessary to estimate vulnerability and risk. It should be mentioned that vulnerability analyses awee done in Arcgis 10.2.2, hazard effects and Risk in Erdas Er mapper 2013, and artwork in CorelDraw X7.

3.1 Hazard

Aida (1978) describes a numerical experiment for tsunami generation based on a seismic fault model, using seismic parameters, and shows that the calculated tsunamis agreed reasonably well with the tsunami records observed at several stations along the coast. He proposes the existence of a correction factor *K* to correct the theoretical values. Since the time of that publication, several different methods to model the seismic source of an earthquake using seismic and geodetic data observed from the earthquake have been proposed (Johnson 1999; Ratnasari et al. 2020; Gusman et al. 2014), as well as different methods to model the displacement of water generated by the seismic source. (Geist 1999; Bryant 2001). In this study, we applied the methodology used in a previous study in Oaxaca, Mexico (Núñez-Cornú et al. 2008), as described below, to model the 1787 earthquake-tsunami effects, as in this case, there was no seismic model of the source. A seismic source based on the local tectonics was proposed; the theoretical tsunami waves modeled fit fairly well with the description of historical damage.

In this case, we assume the rupture will occur on the plate interface and assume dimensions consistent with an M_w ~8.0, which for the Vallarta Gap is an inverse fault plane of L = 150 ± 30 km, W = 60, km, dipping 11° towards the coast at a depth of 10 km on the interplate region, according to the standard relation:

$$\mathrm{M_w} = 2/3 \log_{10}(A) - 10.73 \qquad \textbf{(1)}$$

where *A* is the area in km^2 (Utsu and Seki 1954; Wyss 1979; Singh et al. 1980).. The total area was integrated in segments of individual subareas, $A_i = 30\ x\ 30\ km^2$. Twelve segments were used (Figure 3).

The seismic moment Mo_i of each of the segments was adjusted individually by varying the coseismic dislocation (d_i) from to the relationship

$$\mathrm{Mo_i} = \mu\ \mathrm{A_i}\ \mathrm{d_i} \qquad \textbf{(2)}$$

to fit the moment magnitude of the earthquake (Mw) (Hanks and Kanamori 1979). Moment estimates assume a rigidity modulus

196 $$\mu = 5x10^{11}\ \ dyn/cm^2 \qquad \textbf{(3)}$$

197 which has been used previously for this region by various authors:

198 $$M_w = 2/3\log_{10}(\sum_{i=1}^{12} Mo_i) - 10.73 \qquad \textbf{(4)}.$$

199 The coseismic vertical deformation of the seafloor as produced by the buried fault
200 plane is computed by using the dislocation model of Mansinha and Smylie (1971) by
201 prescribing a reverse fault mechanism on each one of the segments. Increasing the d_i value
202 will increase the value of the Mo_i and the M_w. For the initial tsunami condition, the sea-level
203 change is taken to be the same as the seafloor uplift calculated from the dislocation model.

204 The propagation of the tsunami is simulated by the vertically integrated longwave
205 equations (Pedlosky 1982):

206 $$\frac{\partial \eta}{\partial t} + \overline{\nabla} \cdot M = 0 \qquad \textbf{(5)}$$

207 $$\frac{\partial M}{\partial t} + g\, h\, \overline{\nabla}\ \eta = 0 \qquad \textbf{(6)}.$$

208 In these equations, t is time, η is the vertical displacement of the water surface above the
209 equipotential level, h is the depth of the water column, g is gravitational acceleration, and M
210 is the vector of the discharge fluxes in longitudinal and latitudinal directions. These equations
211 are solved in a spherical coordinate system by the method of finite differences with the Leap-
212 Frog scheme (Goto et al. 1997). For computation, the step time was set to 1 s, and the grid
213 spacing of 27 s was used for the whole region, whereas a grid spacing of 3 s was used to
214 describe the shallow areas. For nearshore bathymetry in the study region, from 1000 m depth
215 to the coast, we used data from local navigational charts (SEMAR 2011). No detailed
216 bathymetry of BdB was available (scale 1:4,000 or high). While for depths greater than 1000
217 m, we used data from the *ETOPO-2* data set (Smith and Sandwell 1997).

218 This model generated theoretical tsunami waveforms and arrival times, which were
219 computed along the coast in 24 virtual gauge sensors (theoretical pressure sensors or VTG)
220 off the coast of the Nayarit, Jalisco, and Colima states, at depths of 10 m (Figure 3). The

tsunami amplification factor because of shoaling from 10 m depth up to the coast is practically negligible and ranges from 1 to 2%. To measure the maximum flood area due to run-up, a digital terrain elevation model (DTM) was generated on land, with cells of 4 m^2, that was interpolated from the DTM obtained by photogrammetry at the year 2000 (Núñez-Cornú et al. 2006). This DTM allows us to map elevation values equivalents to the run-up model. Tsunami hazard calculated for a scenario of maximum flooding in high tide and tsunami's model. Different zones were delimited to match altitude values at Puerto Vallarta's coast with synthetic tsunami waveforms and local tide variation, around +1 m, based on tidal forecasts by Centro de Investigación Científica y de Educación Superior de Ensenada, Baja California (CICESE 2016) for Puerto Vallarta for the years 2012, 2013 and 2016.

3.2 Vulnerability

We follow the same methodologies used by Núñez-Cornú et al. (2006) and Suárez-Plascencia et al. (2008) for the previous city's vulnerability studies, natural hazard's atlas and, disaster's reports in México (Guzman et al. 2003; Simioni 2003; Rosales et al. 2004; García et al. 2014). Extensive information concerning people, homes, and facilities in our study area was available from different online platforms, whether governmental or private because Puerto Vallarta is a city. Data used, such as people and housing, are from different platforms as Consejo Nacional de Población (CONAPO 2012), Instituto Nacional de Estadística y Geografía (INEGI 2010; 2012; 2013; 2015). Some facilities data in the studied area were updated using Google (2015) application.

The analysis in this study consisted of determining population attributes and locations of government offices or facilities that indicate Puerto Vallarta´s vulnerability in the affected area by the local tsunami hazard. We included census information of 214 Basic Geostatistical Areas (AGEB as defined by INEGI) and of five rural localities (less than 2,500 inhabitants, Figure 2) for the whole of Puerto Vallarta county.

According to Guzman et al. (2003), it is necessary to estimate the population affected if the hazard occurs, for that reason the population projection in the affected area to the year 2015 was calculated, assuming that the growth was natural, the following equation was used;

$$C = P(e^{r \cdot t}) \quad (7)$$

where C is the exponential growth of the population susceptible to hazard, P number of inhabitants registered in the last census, e is Euler's number, r is the population growth rate and t is the time in a year, concerning the last available census.

The equation used to project five years after the last available census to know the annual projection data of population growth at the municipal level and assuming that the population grows continuously and slowly, the latter supposes that there are no mass migratory movements after the available census records. The municipality's growth rates for the years 2010 to 2015, calculated by CONAPO (2012), we used in the population projection equation; it was necessary because the following census data will be after the year 2020.

We used a vectorial geographical information system (GIS) to calculate z statistic in population data (Wheather and Cook 2000; Mendenhall et al. 2013), with these values, it was possible to compare different AGEBS per vulnerabilities (attributes) in the affected area. Furthermore, the vulnerability of the population was analyzed according to the age range (Table 2) with different factors or criterion scores (Gómez and Barredo 2006) for prioritizing the vulnerability age group. Only for this information layer and before z statistic was calculated, different experiments were carried out to observe which values highlighted the most vulnerable age groups. High value was for the population less than six years old, followed by older adults and populations with special needs (limited range of motion or learning), with the assumption that in these population categories, support would be needed for transport or with precise instructions to facilitate their movement to a shelter.

Other population attributes are also observed as the type of housing and availability of services such as electricity and potable water services, internet, and computer availability, these do not represent significant differences in affected AGEBs, and therefore they are not used in the final maps.

We also located within the county, the vulnerable facilities that in case of contingency, it is necessary to keep them in operation, like bridges, shopping centers (supply of food), schools, communications, and transportation. Facilities were located in GIS and

277 then were reclassified as high vulnerability. In the same way, we added a layer for overall
278 average damages to household goods for affected tsunami areas. The total vulnerability in
279 each AGEB is evaluated in eight information layers or vulnerability criteria, which are
280 reclassified as very high, high, medium, and low. In this way, a vulnerability is obtained as
281 a basis for calculating risk (Figure 4). The study area is divided into eight micro-basins by
282 natural boundaryies in the vulnerability map.

283 Then we observed results in each AGEB and then we reclass vulnerability ratings as
284 low, mean, or high for local tsunami for Puerto Vallarta City (Figure 4). Layers with z statistic
285 can be viewed as a density distribution, age ranges, education level, range of motion or
286 learning, occupied population and, housing.

287

288 **3.3 Risk**

289 Smith (2013) claims that risk analysis is based on probability theories. When the
290 analysis is undertaken, risk (R), taken as some product of probability and loss. Tobin and
291 Montz (1997), define a hazard as a potential threat to humans and their welfare, and suggest
292 that the risk is expressed as the product of the probability of occurrence (hazard) and
293 vulnerability.

294 To evaluate the risk in Puerto Vallarta, we estimate from the modeling of one
295 earthquake with the initial condition for a tsunami and the vulnerability information
296 previously described, according to the relation:

297 $$\mathrm{R} = \mathrm{H} \times \mathrm{V} \qquad \textbf{(8)}$$

298 where R is risk, H hazard and, V vulnerability.

299 Moreover, the following functions used (Figure 4):

300 $$\mathrm{H(h)} = (\mathrm{run} - \mathrm{up})(\mathrm{probability\ factor}) \qquad \textbf{(9)}$$

301 also, the *probability factor* or dislocation factor is related to the *Mo* or Magnitude, according
302 to logarithmic Gutenberg-Richter relation (Stein and Wysession 2014):

303 $$\log N = a_1 - bM \qquad \textbf{(10).}$$

304 Vulnerability information´s layers reclassified in each AGEB (Figure 4):

305 $$\mathrm{V(v)} = \mathrm{v1} + \mathrm{v2} + \mathrm{v3} + \mathrm{v4} + \mathrm{v5} + \mathrm{v6} + \mathrm{v7} + \mathrm{v8} \qquad \textbf{(11)}$$

306 where *v1* is education, *v2:* housing, *v*3: occupied population, *v*4: age, *v*5: population density,
307 *v*6: the range of motion or learning, *v*7: facilities and, *v8:* clean debris.

308 For the inhabited homes in the tsunami flood area, costs for the loss of household,
309 cleaning, and debris transportation were calculated for each micro-basin. For this, a program
310 is used to budget costs and control civil engineering work. The damage costs do not estimate
311 the structural damages to buildings or bridges caused by a high magnitude earthquake. Nor
312 do we include the costs associated with the cessation of day-to-day operations for an
313 international airport, international maritime terminal, and regional bus station, which we
314 excluded from this study. Also we excluded the costs for the loss of cultural heritage, such
315 as Museo del Cuale (sometimes unrecoverable as an archaeological site), or costs such as the
316 loss of documents in cadaster, special equipment or computer in hospitals, government
317 offices, and schools.

318 The risk and vulnerability maps were generated in a raster image manager, for which
319 values for Puerto Vallarta were entered at different points in each AGEB and interpolated
320 with a spline method.

321

4 Results

4.1 Earthquake, fracture area, magnitude, and dislocation

In this study, different tests were performed for the proposed tsunami by changing the initial earthquake conditions by varying the dislocation while keeping the fracture plane constant. In this work, five hazard scenarios were evaluated with dislocation values d_i = 2, 3, 4, 5, and 6 m (Table 3) for Puerto Vallarta. Pitillal riverside (VTG 5, Figure 3 and Figure 5) was the site of the highest run-up calculated along Puerto Vallarta coast, 2.7 m ≤ *Hr* ≤ 8 m, and I_t = 20 min, A_t = 72 min. We analyze, in particular, the case for d_i = 5m.

4.2 Sea level and arrival times

The tsunami hazard was obtained from run-up values that affected Puerto Vallarta. We calculated a scenario for maximum flooding assuming the Mw 8.0 earthquake occurred at high tide and run-up would affect coastal communities in our study region. The synthetic tsunami waveforms outputs generated for the first 10 hours after the earthquake for 24 VTG distributed on the southern coast of Nayarit, Jalisco, and north of Colima, heights, and arrivals times of tsunami for coastal communities for the studied region are plotted in Figure 5 and listed in Table 4.

In Jalisco coast, the calculated first Tsunami wave (*Hi*) had an arrival time (*It*) of 11 min after the earthquake, and corresponded to the municipality of Cabo Corrientes for the VTG near communities Aquiles Serdán (*Hi* = 5.8 m, *It* = 11 min) and Ipala (*Hi* = 9.0 m, *It* = 13 min). At Ipala the Run-up wave (*Hr*) is 10.9 m and the arrival times (*At*) 37, 60, 96, and 120 min (in this case four “big” waves were generated) (Table 4). In Tomatlán, for the marsh zones of Colorado and Majahuas, *Hi* = 6.1 m, *It* =19 min. At Chamela (La Huerta), *Hr* = 5.1 m and *At* = 61 and 307 min, while at Cihuatlán (San Patricio) *Hr* = 2.2 m and *At* = 106 min. In Bahía de Manzanillo, Colima *Hr* = 3.9 m and *At* = 177 min. Meanwhile, to the north at La Cruz de Huanacaxtle in BdB (Nayarit) ,*Hr* = 7.0 m and *At* = 86 min.

4.3 Flood by a local tsunami

The Hr and the most ocean water inland penetration (x) were calculated for our region. Five of eight micro-basins tsunami hazard scenarios were at the maximum, with a run-up of 5 m $\leq Hr \leq$ 9 m and an inland penetration of 0.6 km (Cuale) $\leq x \leq$ 5.1 km (Ameca), resulting in a total flood area of 30.55 km^2. The tsunami flood and Hr comparison between micro-basins Ameca, Salado, Pitillal, Camarones, and Cuale are shown in Figure 6. Significant flood volume by the tsunami wave was estimated in the Salado estuary area, where the elevation is 1 m below sea level.

4.4 Housing and public facilities vulnerability

In 2010, Puerto Vallarta had 255,681 inhabitants, 96% of which was concentrated in the study area. The remaining people for the municipality live in ≥ 100 rural towns whose elevations are ≥ 20 m. For that reason, the rural towns were not considered in the risk assessment because they are outside the areas directly affected by the local tsunami hazards. By the year 2015, this study calculated that the population in the flood area increases to include 47 AGEB as shown in Figure 7. This is gives by equation $C = P(e^{r \cdot t})$ = 88,316 inhabitants inside the adverse effects of natural hazards.

Land use in Puerto Vallarta has favored the establishment of tourist services, commerce, and high-density housing close to the beach. For the year 2010, there were 33,942 dwellings in the affected area, of which 23,271 inhabited. The services available such as potable water, electricity, and drainage between the tourist strip and the rest of the community were compared. It is observed that the indexes are similar in the all municipalities, even in zones of height greater than 20 m, the reason is that there is an acceptable comparable coverage of these services. In the case of a disaster in Puerta Vallarta, it is assumed that the first attention would be given to re-establish services to the tourist zone. The most significant proportion of vulnerable housing in the study area is distributed in the Salado and Pitillal micro-basins.

At the time of this study, there were 320 vulnerable public facilities in the municipality, of which 33% are vulnerable to flooding if a local tsunami occurs. Table 5

shows the number of public facilities and the volume of debris per micro-basin to estimate cleaning costs. The number of vulnerable facilities observed by micro-watersheds is as follows: 45 in Salado, 27 in Pitillal, 14 in Cuale, 12 in Ameca-Mascota, and 6 in Camarones. The percentages of vulnerable facilities for the total municipality considering their primary use are the following: schools 15%, government and emergency care 5%, health units 2%, and for various uses 11% (such as the distribution of electric energy, fuel storage, shopping malls, entertainment, museums, roads, transportation, and bridges).

For the vulnerability categories, the z statistic was used; they classified as NULL for the case that in the AGEB, the data is equal to zero or data not available. The low vulnerability group corresponds to the values $z \leq -0.5$, medium for values $-0.5 < z < 1$, and high for values of $z > 1$. Different ranges of z-score values were established in layers of education level, occupied population, and housing by observing in the study area those values that reflect the conditions of hypothesis.

High vulnerability values due to population variables such as age or special needs (physical or learning), educational condition, and population density were observed at the El Salado, Pitillal, and Ameca micro-basins (Las Juntas). The total occupied population of the municipality of Puerto Vallarta in 2010 was 47,676, of which 18,592 are in the tsunami impact zone, and are concentrated in the El Salado basin. We use a raster GIS for the image to show the vulnerability map of Puerto Vallarta for the local tsunami hazard as far as an elevation of 30 m. Its map was obtained from 539 points with all the municipality´s information, of which 219 points correspond to AGEB with data for population and housing data and 323 points for the vulnerable facilities (Figure 8).

4.5 Risk

We estimated the cost of property damage in each dwelling inhabited in the affected area under the assumption that the minimum damage was $1,200 US dollars (which includes damage to some household goods as living room, breakfast room, bed, and kitchen), so the total cost calculated for this concept was $27,925,200 US dollars.

Cleaning and transporting debris costs depend on the volume calculation. The affected areas were measured in each micro-basin, assuming a debris height of 0.1 m. The condition established that the debris was vegetation, sand, and mud and that people should do the cleaning without the use of special equipment. For debris moving and unloading costs, the conditions were to use a dump truck and to transit by road up to a distance of 1 km. The cost calculated for this concept was $6,457,899 US dollars (Table 5).

We used a raster GIS for imaging to show the risk in Puerto Vallarta for a local tsunami, and focused in five of eight micro-basins: Ameca, Salado, Pitillal, Camarones and, Cuale, where the observed land uses were the hotel zone with medium risk, the housing area and the vital facilities with high and very high risk. We present two maps of Risk: in the first (Figure 9a), we consider the total flood area due to a 5m coseismic slip; in the second (Figure 9b), an empirical probability factor based on the magnitude (coseismic slip) was considered; a smaller slip is more likely than a large slip, in this case, a probability factor between 1.0 and 0.1 (Figure 4) was applied to the vulnerability.

5 Discussion

We calculated *Hr* and At for local tsunami to assess the hazard on Jalisco's and southern Nayarit´s coasts using a theoretical seismic source based on the local tectonics. Values used for the coseismic slip or dislocation range from two to six meters ($8.0 < Mw < 8.2$). Pacheco et al. (1997) propose a maximum slip of 4 m for the 1995 earthquake. Quintanar et al. (2011) proposes a maximum slip of 3.2 m for the 2003 earthquake, however, there is no reported tsunami for this earthquake. Trejo et al. (2015) use the same method to model the effects of the 1995 earthquake tsunami, but use different slips in some segments of the

428 rupture area to adjust the reported data (Ortiz et al. 1995). The *Hr* estimated in five places of
429 Puerto Vallarta coincides with the studies of Nuñez-Cornú et al. (2006), Dresler, and Nuñez-
430 Cornú (2007). The scales of the data do not allow for the estimation of a tsunami due to the
431 slipping of sediments in the deltas of the rivers in Puerto Vallarta, as happened in Coyutlan,
432 1932. For this tsunami we estimated more significant destruction because the *Hr* was ≥ 10 m
433 because of the earthquake's impulse due to the collapse of the sediment fringe of the Armeria
434 River after an earthquake of magnitude $M = 6$ (Núñez-Cornú-Cornú 2011).

435 Previously, these types of studies have not been carried out in Mexico, the evaluation
436 of vulnerability for tsunamis and the methodology used in this study is similar to that used
437 for floods and earthquakes hazards, the population, and facilities affected at the moment of
438 hazard occurs (Guzman et al. 2003). These studies are based on the information available for
439 the city of Puerto Vallarta and published by government agencies. Some previous studies as
440 the Natural Hazards Atlas and Ecological Planning Program or the Integrated Management
441 of Coastal Landscapes (Nuñez-Cornú et al. 2006; Núñez-Cornú and Carrero 2012). The
442 methodology seemed appropriate considering the available information as a whole and could
443 be analyzed in a GIS. The vulnerability of the municipality of Puerto Vallarta estimated by
444 tsunami flooding be useful for both the local or regional type following a major earthquake
445 or a distant one in the case that the tsunami would enter the bay with an amplitude equal to
446 the natural frequency of BdB which could then generate seiches. The results provide some
447 preliminary answers for this particular city, and we did not consider the floating population
448 due to tourism because it varies by the time of year and the characteristics of the hotel,
449 quality, and service costs. However, this study represents the first approximation of
450 estimating municipality vulnerability, with ≥ 275,640 people living in this city (IIEG, 2018),
451 which will improve with the availability of the data from the next census in 2020.

452 Puerto Vallarta is a medium-sized city, and we did not assess the vulnerability of
453 buildings (Simioni 2003; Santos et al. 2014; Voulgaris and Murayama 2014) only the surface
454 area affected by tsunami flooding. In our case study, land use is mostly designated for
455 buildings, hotels, tourist services, and commerce and these are closest to the coast. Regarding
456 hotels are > 4 levels (susceptible to respond to vibration by the earthquake energy), we

457 worked with two assumptions, (a) low tsunami´s velocity does not generate too much
458 turbulence as Tenacatita bay, October 1995 and (b) buildings are seismo-resistant so they
459 would not collapse. Given these conditions, in some places in Puerto Vallarta, multi-story
460 hotels could serve as vertical evacuation and shelter for the guests themselves in the case of
461 a tsunami.

462 In other places, moving to a safe area is more feasible. We observed theoretical
463 tsunami travel results from some places in the study area. Walking to a safe area is feasible
464 in 11 minutes or 16 min if walking speed (v) is 1.1 m/s or if under severe walking conditions
465 $v = 0.751$ m/s (Ashar et al. 2018), because our model estimated that the first tsunami arrival
466 would be at ≥ 19 minutes (Table 4 and Figure 6). It is important not to forget that a family
467 emergency plan is essential for people with special needs (support is needed as transport or
468 precise instructions to facilitate their movement to a shelter).

469 Storm surge inundation in Puerto Vallarta has happened previously An example of
470 flood damage was a storm surge generated by Hurricane Kenna in October 2002. The waves
471 produced by this hurricane entered land up to a distance of 1 km approximately. Three hotels
472 suffered intense non-structural damage, and the tourist strip was affected with different levels
473 of damage depending on the proximity to the beach, or due to flooding and sand depostion.
474 There were no reported direct victims associated with this hazard at Puerto Vallarta. To assess
475 tsunami risk in Puerto Vallarta, the vulnerability was analyzed by criteria scores (Gómez and
476 Barredo 2006), and hazard by probability factor (dislocation factor) according to the height
477 at the study area and some parameters of local (this study) or tele-tsunami calculated by
478 Dressler and Nuñez-Cornú (2007).

479

480 **6 Conclusions**

481 Puerto Vallarta is located in a seismic region, in which great magnitude earthquakes
482 and local tsunamis have occurred. In this city, the impact due to historical tsunamis is
483 unknown due to a lack of evidence because to date no specific studies have been carried out.
484 However, the results presented in this work are useful in protocols and to civil defense in

485 Jalisco and provides essential information for the county´s territory managers, which design
486 one Partial Development Plan. A preliminary evaluation of essential cost damage for a
487 simplified house and for the cleaning of debris was also calculated. Maps for tsunami hazard
488 and local vulnerability in Puerto Vallarta were made.

489 The risk area in Puerto Vallarta County State affected by flooding due to a local
490 tsunami was measured to be 30.55 km^2 approximately. The highest risk was found in the
491 northern study area, between the valleys of the Ameca and Pitillal rivers (calculated area 26.5
492 km^2), because this area containts the greatest population density at Puerto Vallarta and at a
493 distance of 0.8 km from the coastline, also there a regional bus station, an international
494 airport, and an international port. We consider that the northern hotel zone could be a vertical
495 evacuation zone for tourists and local people, following the such an earthquake and tsunami.
496 Some hotels in Puerto Vallarta could function as a refuge; these seismically resistant
497 structures should have more than six levels. One factor that increases the risk created by a
498 local tsunami in the Puerto Vallarta coastal strip is the current land use. It has allowed a
499 reduction in protective zones, and high population density construction close to the beach,
500 and in the zones of mangroves in the Ameca and Salado micro-basins. While in the south
501 study zone, from Boca de Tomatlán community to Playa Camarones, the risk area is 1.5 km^2,
502 and it is feasible for people to walk to a safe area from some points, as an example in
503 Camarones micro-basin people should walk toward the south to the municipal stadium. For
504 this, it is necessary to do some preliminary evacuation tests to determine escape routes and
505 keep people safe for at least four to six hours, because the arrival time for the second wave
506 was calculated by the model as on hour after the tsunami. This second wave arrival time is
507 micro-basin dependent.

508 The perception of the appropriate hazard in the minds' of the managers of the Jalisco
509 State will guarantee that economic and social activities are sustainable. It is suggested that
510 the next partial plans of county development are reviewed, specifically the strip of coastline
511 of up to 20 m elevation in Jalisco State, such that land use favors very low population density
512 and the implementation of a construction standard for seismo-resistant buildings throughout
513 this county.

514 **Acknowledgements**

515

516

517 **References**

518

519 Aida I (1978) Reliability of a Tsunami Source Model Derived from Fault Parameters. J. Phys.
520 Earth 26: 57-73
521 Allan J F, Nelson S A, Luhr J F, Carmichael I S E, Wopat M, Wallace P J (1991) Pliocene-
522 recent rifting in SW México and associated volcanism: An exotic terrane in the
523 making. American Association of Petroleum Geologists, Memoir 47: 425–445
524 Ashar F, Amaratunga D, Haigh R (2018) Tsunami Evacuation Routes Using Network
525 Analysis: A case study in Padang. Procedia Engineering 212: 109–116.
526 https://doi.org/:10.1016/j.proeng.2018.01.015
527 Bourgois J, Renard D, Auboin J, Bandy W, Barrier E, Calmus T, Carfantan J C, Guerrero J,
528 Mammerickx J, Mercier de Lepinay B, Michaud F, S R (1988) Fragmentation en
529 cours du bord Ouest du Continent Nord Americain: Les frontières sous-marines du
530 Bloc Jalisco (Mexique). Comptes Rendus Académie Des Sciences 307(II): 1121–
531 1130
532 Bryant E (2001) Tsunami, The Underrated Hazard. Cambridge University Press, Cambridge
533 Centro de Investigación Científica y de Educación Superior de Ensenada (CICESE), 2016.
534 Calendarios mensuales predicción de mareas [online]. Ensenada: Centro de
535 Investigación Científica y de Educación Superior de Ensenada. Available from:
536 http://predmar.cicese.mx/calendarios/
537 Consejo Nacional de Población (CONAPO), 2012. Proyecciones de la población por
538 Municipio 2010-2030 [online]. México. Available from:
539 http://www.conapo.gob.mx/es/CONAPO/Proyecciones_Datos
540 Dañobeitia J, Bartolomé R, Prada M, Nuñez-Cornú F J, Córdoba D, Bandy W L, Estrada F,
541 Cameselle A L, Nuñez D, Castellón A Alonso, J L, Mortera C, Ortiz M (2016)
542 Crustal Architecture at the Collision Zone Between Rivera and North American

543 Plates at the Jalisco Block: Tsujal Project. Pure and Applied Geophysics 173(10–11):
544 3553–3573. https://doi.org/:10.1007/s00024-016-1388-7
545 DeMets C, Stein S (1990) Present-day kinematics of the Rivera Plate and implications for
546 tectonics in southwestern Mexico. Journal of Geophysical Research 95(B13) 21: 931-
547 948. https://doi.org/10.1029/JB095iB13p21931
548 Dixon T H (2015) Ten Years after Katrina: What Have We Learned? Eos: 96.
549 https://doi.org/10.1029/2015EO034703. Accessed 27 August 2015
550 Dressler R, Núñez-Cornú F J (2007) Estudio de la marea M2, del efecto de tsunamis y de
551 campos de Viento en Bahía de Banderas, México, mediante un modelo hidrodinámico
552 númerico (in Spanish). Geos 27(1): 100
553 García Arróliga R, Marín Cambranis K, Méndez Estrada N, Troncoso Arriaga (2014)
554 Resumen de los efectos de los desastres ocurridos en 2010. In: García Arróliga R,
555 Marín Cambranis K, Méndez Estrada N, Troncoso Arriaga (eds) Características e
556 impacto socio-económico de los principales desastres ocurridos en la República
557 Mexicana en 2010. CENAPRED, México, pp 9–18
558 Garduño V H, Tibaldi A (1991) Kinematic evolution of the continental active triple junction
559 of the western Mexican Volcanic Belt. Comptes Rendus Académie Des Sciences
560 312(II): 135–142
561 Geist E L (1999) Local Tsunamis and Earthquake Source Parameters. In: Dmowska R,
562 Saltzman B (eds) Advances in Geophysics 39: Academic Press, Cambridge, pp 117-
563 209
564 Gómez Delgado M, Barredo Cano J I (2006) Evaluación multicriterio y multiobjetivo en el
565 entorno de los sistemas de información geográfica. In: Gómez Delgado M, Barredo
566 Cano J I (eds) Sistemas de Información Geográfica y evaluación multicriterio en la
567 ordenación del territorio. Alfaomega Grupo Editor S A de C V, México, pp. 43–76
568 Goto C, Ogawa, Y, Shuto N, Imamura F, (1997). IUGG/IOC Time Project: numerical method
569 of tsunami simulation with the leap-frog scheme 126. UNESCO, New York.
570 https://unesdoc.unesco.org/ark:/48223/pf0000122367. Accessed June 2015

571 Gusman A R, Tanioka Y, Macinnes B T, Tsushima H (2014) A methodology for near-field
572 tsunami inundation forecasting Application to the 2011 Tohoku tsunami. Journal of
573 Geophysical Research Solid Earth 119: 8186–8206
574 Guzman J M, Silva A, Poulard S, Jovel R (2003) Segunda parte sectores sociales, población
575 afectada. In: R Zapata Martí and Jovel, (eds) Manual para la evaluación del impacto
576 socioeconómico y ambiental de los desastres LC/MEX/G5 Naciones Unidas
577 Comisión Económica para América Latina y el Caribe, México, pp. 29–66
578 https://repositoriocepalorg/handle/11362/2781 . Accessed June 2015
579 Hanks, T C, and Kanamori, H (1979) A moment magnitude scale. Journal of Geophysical
580 Research 84(B5): 2348. https://doi.org/101029/JB084iB05p02348
581 Hebenstreit GT, Gonzalez FI, JPreus (2003) Tsuami Impact and Mitigation in Inhabited
582 Areas. In: G Heiken, Fakunddiny and Sutter (eds) Earth Science in the City A Reader,
583 American Geophysical Union: Washington DC, pp. 171-186
584 Instituto Nacional de Estadística, Geografía e Informática (INEGI) (2010) Censo de
585 Población y Vivienda 2010, principales resultados por AGEB y manzana.
586 http://wwwinegiorgmx/est/contenidos/proyectos/ccpv/cpv2010/Defaultaspx
587 Accessed June 2015
588 Instituto Nacional de Estadística, Geografía e Informática (INEGI) (2012) Directorio
589 Estadístico Nacional de Unidades Económicas (DENUE) 2012.
590 http://www3inegiorgmx/sistemas/mapa/denue/defaultaspx Accessed June 2015
591 Instituto Nacional de Estadística, Geografía e Informática (INEGI) (2013) Inventario
592 Nacional de Viviendas. http://www3inegiorgmx/sistemas/mapa/inv/defaultaspx
593 Accessed June 2015
594 Instituto Nacional de Estadística, Geografía e Informática (INEGI) (2015) Encuesta
595 intercensal 2015
596 http://wwwbetainegiorgmx/proyectos/enchogares/especiales/intercensal/ Accessed
597 June 2015
598
599
600

Instituto Nacional de Estadística, Geografía e Informática (INEGI) (2020) Censo de Población y Vivienda 2020, Población total. https://www.inegi.org.mx/sistemas/Olap/Proyectos/bd/censos/cpv2020/pt.asp. Accessed 22 April 2021

Johnson J M (1999) Heterogeneous Coupling along Aaska-Aleutians as Inferred from Tsunami, Seismic and Geodetic Inversions. Advances in Geophysics 39, Academic Press: Cambridge

Luhr J, Nelson S, Allan J, Carmichael I (1985) Active rifting in southwestern México: manifestations of an incipient eastward spreading-ridge jump. Geology 13: 54–57

Mansinha L, Smylie D E (1971) The displacement fields of inclined faults. Bulletin of the Seismological Society of America 61(5): 1433–1440

Mendenhall W, Beaver R J, Beaver B M (2013) Data descriptions with numerical measures. In: J H Romo Muñoz and A E García Hernández (eds) Introduction to Probability and Statics, 13th ed. CENGAGE Learning,: México, pp. 52–93

Mileti D S, Bolton P A, Fernandez G, Updike R G (1991) The Eruption of Nevado Del Ruiz Volcano Colombia, South America, November 13, 1985. The National Academies of Sciences, Engineering and Medicine: Washington, DC

Núñez-Cornú F J (2011) Peligro Sísmico en el Bloque de Jalisco, México. Física de La Tierra 23(0): 199–229. https://doi.org/105209/rev_FITE2011v2336919

Núñez-Cornú F J, Carrero-Roa M (2012) III Fragilidad. In: F J Núñez Cornú, Rodríguez Gutierrez, R M Chávez Dagostino (eds) Gestión integrada de paisajes litorales Hacia una metodología comparativa caso Asturias y Bahía de Banderas México, Plaza y Váldez Editores, México, pp. 93–141

Núñez-Cornú F J, Córdoba D, Dañobeitia J J, Bandy W L, Figueroa M O, Bartolome R, Nuñez D, Zamora-Camacho A, Espindola J M, Castellon A, Escudero C R, Trejo-Gomez E, Escalona-Alcazar J, Suarez Plascencia C, Nava F A, Mortera C, TsuJal Working Group 2016 Geophysical Studies across Rivera Plate and Jalisco Block, Mexico: TsuJal Project. Seismological Research Letters 87(1): 59–72. https://doi.org/101785/0220150144

Núñez-Cornú F J, Ortiz M, Sánchez J J (2008) The great 1787 Mexican tsunami. Natural Hazards 47(3): 569–576. https://doi.org/101007/s11069-008-9239-1

Núñez-Cornú F J, Sandoval J M, Alarcón E, Gómez A, Suárez-Plascencia C, Núñez D, Trejo-Gomez E, Sánchez Mariscal O, Candelas Ortiz J G, Zúñiga-Medina L M (2018) The Jalisco Seismic Accelerometric Telemetric network (RESAJ). Seismological Research Letters 89(2A): 363–372. https://doi.org/101785/0220170157

Núñez-Cornú F J, Suárez-Plascencia C, Chavez-Dagostino R M (2006) Informe técnico de caracterización y análisis del subsistema natural de Puerto Vallarta: Atlas de peligros naturales y Programa de Ordenamiento Ecológico Puerto Vallarta, Ayuntamiento de Puerto Vallarta y Secretaría de Desarrollo Social (Programa HABITAT), DOP-068/2006

Orozco and Berra J (1888) Efemérides Sísmicas Mexicanas. Mem Soc Cientif "Antonio Alzate", I-11, México

Ortiz M, González J I, Reyes J, Nava C, Torres E, Saenz G, Arrieta J (1995) Informe técnico efectos costeros del tsunami del 9 de octubre de 1995 en la costa de Colima y Jalisco. CICESE, Ensenada

Ortiz M, Kostoglodov V, Singh S K, Pacheco J (2000) New constraints on the uplift October 9, 1995, Jalisco-Colima earthquake (Mw 8) based on the analysis of tsunami records at Manzanillo and Navidad, Mexico. Geofísica Internacional 39 (4): 349–357

Pacheco J, Singh S K, Domínguez J, Hurtado A, Quintanar L, Jiménez Z, Yamamoto J, Gutierrez C, Santoyo M, Bandy W L, Guzmán M, Kostoglodov V, Reyes G, Ramírez C (1997) The October 9, 1995 Colima-Jalisco, Mexico Earthquake (Mw 8): An aftershock study and a comparison of this earthquake with those of 1932. Geophysical Research Letters 24(17): 2223–2226. https://doi.org/101029/97GL02070

Pedlosky J (1982) Geophysical Fluid Dynamics. Springer-Verlag, Berlin https://doi.org/101007/978-3-662-25730-2

Quintanar L, Rodríguez-Lozoya H, Ortega R, Gómez-González J, Dominguez T, Javier C, Alcantara,L and Rebollar C (2011) Source Characteristics of the 22 January 2003 Mw = 75 Tecomán, Mexico, Earthquake:New Insights. Pure Appl Geophys 168: 1339–1353. https://doi.org/101007/s00024-010-0202-1

660 Ratnasari R N, Tanioka Y, Gusman AR (2020) Determination of Source Models Appropriate
661 for Tsunami Forecasting: Application to Tsunami Earthquakes in Central Sumatra,
662 Indonesia. Pure Appl Geophys 177: 2551–2562 https://doi.org/101007/s00024-020-
663 02483-3
664 Rosales Gómez J, et al, (2004) Guía metodológica para la elaboración de atlas de peligros a
665 nivel ciudad México: Secretaría de Desarrollo Social (SEDESOL) and Consejo de
666 Recursos Minerales (COREMI) http://bibliotecadigitalimipensorg/uploads/Guia
667 metodologica para la elaboracion de atlas de pel ciudadpdf Accessed June 2015
668 Sánchez Devora A J, Farreras-Sanz A J (1993) Catalog of tsunamis on the Western Coast of
669 México, Publication SE-50 S F National Geophysical Data Center, National Oceanic
670 and Atmospheric Administration, Intergovernmental Oceanographic Commission,
671 World Data Center A, Secretaría de Marina de México, Consejo Nacional de Ciencia
672 y Tecnología de México and Centro de Invetigación.
673 https://wwwngdcnoaagov/hazard/data/publications/Wdcse-50pdf Accessed June
674 2015
675 Santos A, Tavares A O, Emidio A (2014) Comparative tsunami vulnerability assessment of
676 an urban area: An analysis of Setúbal city, Portugal. Applied Geography 55: 19–29.
677 https://doi.org/101016/japgeog201408009
678 Secretaría de Marina y Armada de México (SEMAR), 2011 Catálogo de Cartas y
679 Publicaciones Náuticas México pp61 Available from:
680 http://wwwsemargobmx/publicaciones/catalogo/catalogopdf Accessed September
681 2020
682 Simioni D (2003) Planificación y vulnerabilidad urbana. In: D Balbo, Marcelo Jordán,
683 Ricardo Simioni (eds) La Ciudad Inclusiva. Naciones Unidas, Comisión Económica
684 para América Latina y el Caribe (CEPAL), Santiago de Chile, pp. 279–304.
685 https://repositoriocepalorg/handle/11362/27814 Accessed June 2015
686 Singh S K, Bazan E, Esteva L (1980) Expected earthquake magnitude from a fault. Bulletin
687 of the Seismological Society of America 70(3): 903–914

688 Singh S K, Ponce L, Nishenko S E (1985) The great Jalisco, Mexico earthquakes of 1932:
689 Subduction of the Rivera Plate. Bulletin of the Seismological Society of America 75
690 (1): 301-313
691 Singh S K, Rodriguez M, Espindola J M (1984) A catalog of Shallow Earthquakes of Mexico
692 from 1900 to 1981. Bulletin of the Seismological Society of America 74 (1): 265–
693 279
694 Smith K (2013) Environmental hazards: assessing risk and reducing disaster, 6th ed,
695 Routledge Taylor and Francis Group, New York
696 Smith W H F, Sandwell D T (1997) Global Sea Floor Topography from Satellite Altimetry
697 and Ship Depth Soundings. Science 277(5334): 1956-1962.
698 https://doi.org/101126/science27753341956 Accessed June 2015
699 Stein S, Wysession M (2014) Earthquake statics. In: S Strein, M Wysession (eds) An
700 introduction to seismology, earthquakes, and earth structure, Blackwell Publishing
701 Ltd, United Kindom, pp. 274-282
702 Suárez-Plascencia C, Guillen-Patiño K, Núñez-Cornú F J (2008) Riesgo por inundaciones en
703 el sector sur del municipio de Guadalajara. Geos 28(2): 254
704 Suter M (2018) The October 2 1847 MI 57 Chapala Graben Triggered Earthquake (Trans-
705 Mexican Volcanic Belt, West-Central Mexico): Macroseismic Observations and
706 Hazard Implications. Seismol Res Lett 89 (1) https://doi.org/101785/0220170101
707 Suter M (2019) The 1563 MI 8 Puerto de la Navidad Subduction-Zone and 1567 Mw 72
708 Ameca Crustal Earthquakes (Western Mexico): New Insights from Sixteenth-Century
709 Sources. Seismol Res Lett 90 (1) https://doi.org/101785/0220180304
710 Tobin G A, Montz B E (1997) Risk Assessment. In: G A Tobin, (ed) Natural Hazards:
711 explanation and integration, 1st The Guilford Press, New York, pp.281-319
712 Trejo-Gómez E, Ortiz M, Núñez-Cornú F J (2015) Source Model of the October 9, 1995
713 Jalisco-Colima Tsunami as constrained by field survey reports, and on the numerical
714 simulation of the tsunami. Geofísica Internacional, 54(2): 149–159.
715 https://doi.org/101016/jgi201504010
716 Urías Espinosa J, Bandy W L, Mortera Gutiérrez C A, Núñez-Cornú F J, Mitchell N C (2016
717) Multibeam bathymetric survey of the Ipala Submarine Canyon, Jalisco, Mexico

718 (20°N): The southern boundary of the Banderas Forearc Block?. Tectonophysics 671:
719 249–263 https://doi.org/101016/jtecto201512029
720 Utsu T, Seki A (1954) A relation between the area of aftershock region and the energy of
721 main shock. Journal of the Seismological Society of Japan 7: 233–240
722 Voulgaris G, Murayama Y (2014) Tsunami vulnerability assessment in the Southern Boso
723 Peninsula, Japan. International Journal of Disaster Risk Reduction 10: 190–200.
724 https://doi.org/101016/jijdrr201408001
725 Wheater C P, Cook P A (2000) Using statics to Understand the Enviroment. Routledge,
726 London, p. 246
727 Wyss M (1979) Estimating maximum expectable magnitude of earthquakes from fault
728 dimensions. Geology 7(7): 336–340. https://doi.org/101130/0091-7613(1979)

Figures

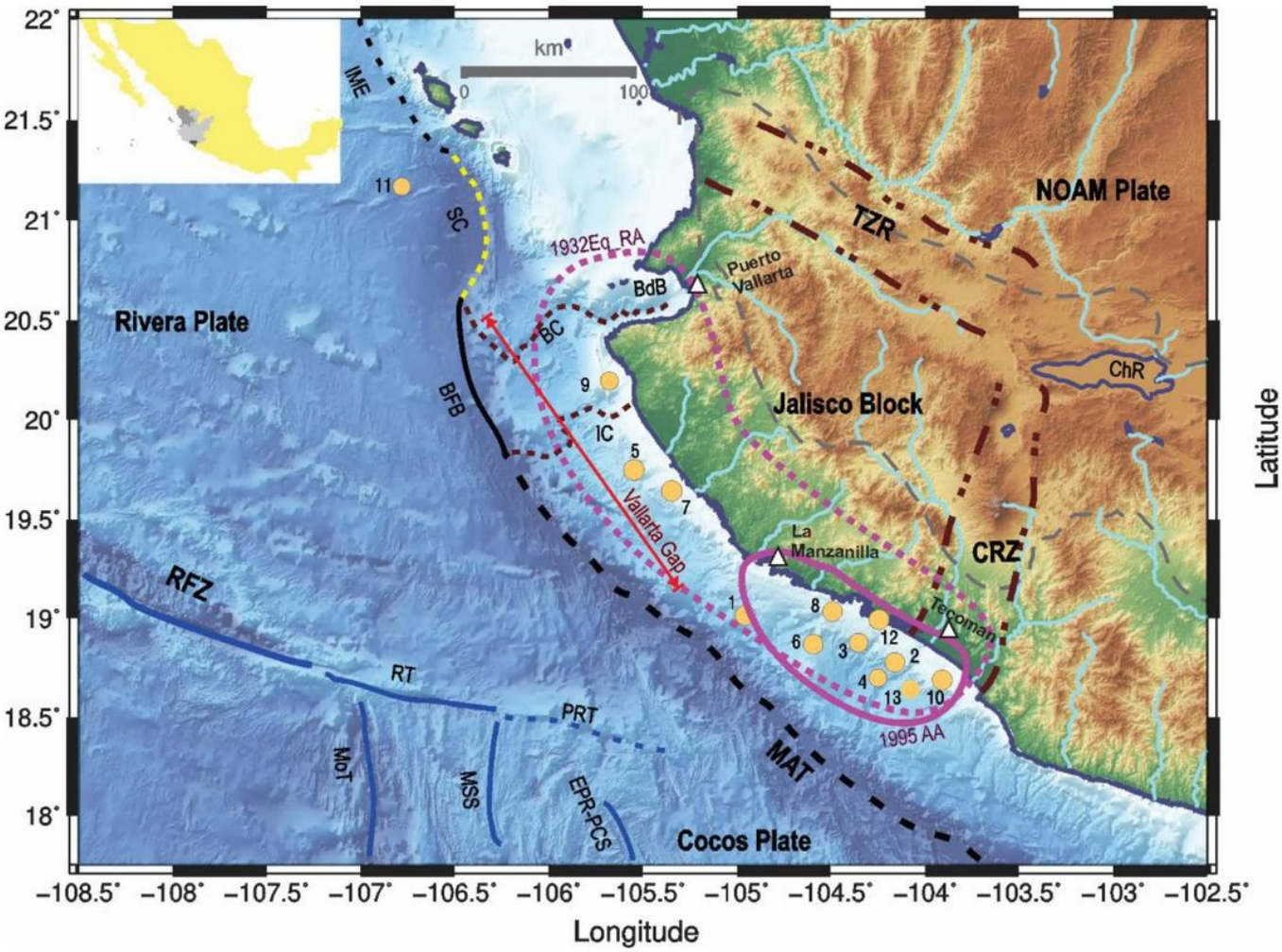

Figure 1

Tectonic framework of the Jalisco region, IME: Islas Marias Escarpment; SC: Sierra de Cleofas; BFB: Bahía de Banderas fore-arc Block; TZR: Tepic-Zacoalco Rift zone; ChR: Chapala Rift zone; CRZ: Colima Rift zone; MG: Manzanillo Graben; MAT: Middle America Trench; RFZ: Rivera Fault zone; MoT: Moctezuma Trough; MSS: Moctezuma Spreading Segment; EPR-PCS: East Pacific Rise Pacific-Cocos Segment; RT: Rivera Transform Fault; PRT: Paleo Rivera Transform fault (after Perez-Gaviria et al. (2013); IME: Islas Marías escarpment; SC: Sierra de Cleofas; BC: Banderas Canyon; IC: Ipala Canyon; BFB: Banderas Forearc Block; BdB: Bahia de Banderas; 1932Eq_RA: Rupture area proposed for 1932 Earthquakes (Singh et al., 1985); 1995 AA: Earthquake Aftershock area. Yellow circles mark the epicenters of the earthquakes in Table 1. Modified from Núñez-Cornú et al. (2018). Note: The designations employed and the presentation of the material on this map do not imply the expression of any opinion whatsoever on the part of Research Square concerning the legal status of any country, territory, city or area or of its

authorities, or concerning the delimitation of its frontiers or boundaries. This map has been provided by the authors.

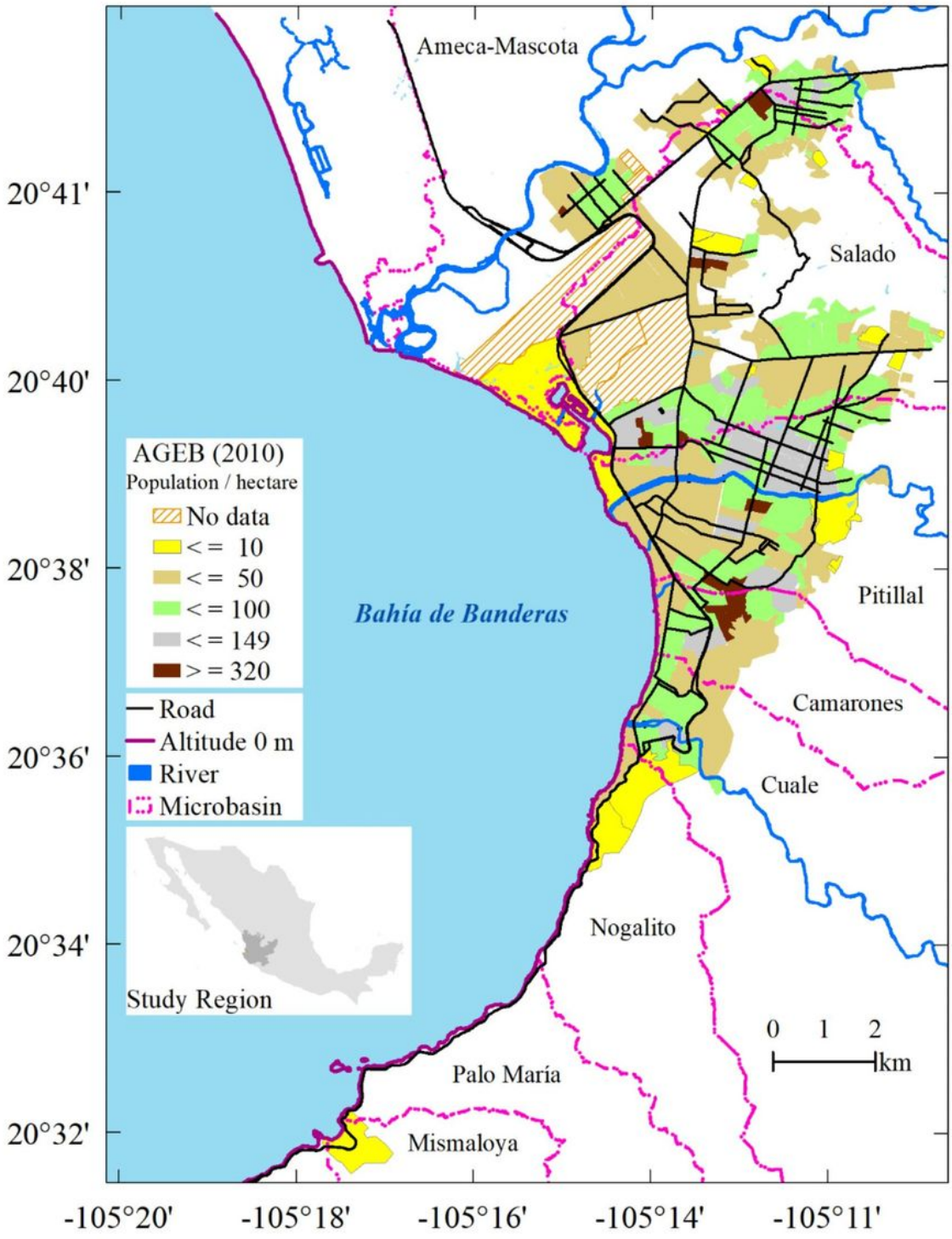

Figure 2

Study area with population density distribution using AGEBs. Note: The designations employed and the presentation of the material on this map do not imply the expression of any opinion whatsoever on the part of Research Square concerning the legal status of any country, territory, city or area or of its

authorities, or concerning the delimitation of its frontiers or boundaries. This map has been provided by the authors.

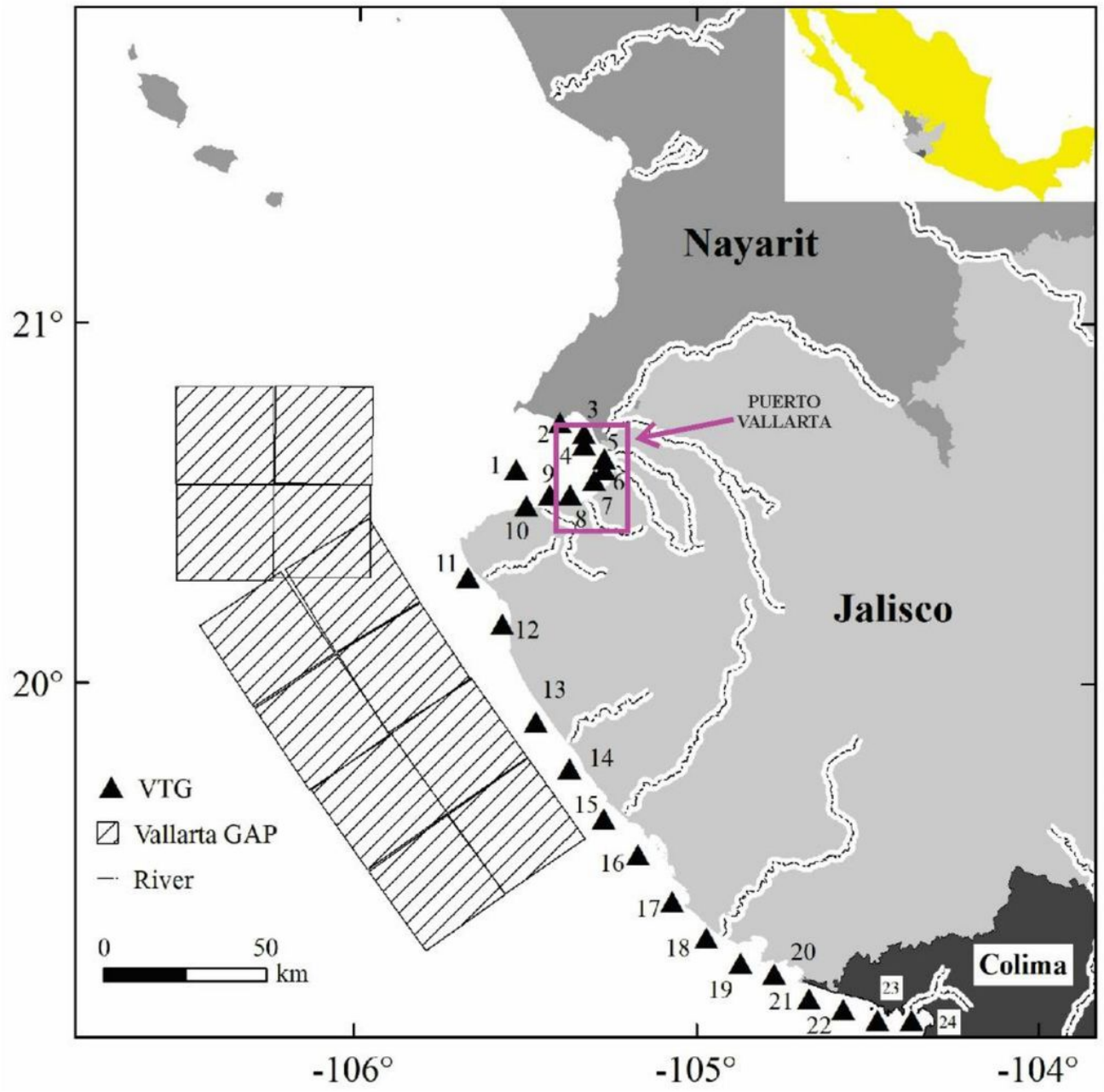

Figure 3

Distribution of rupture area and subareas (rectangles) used to numerically model the local tsunami. Triangles indicate the distribution of virtual gauge sensors (VTG). Numbers indicate the localities, as in Table 4. Note: The designations employed and the presentation of the material on this map do not imply the expression of any opinion whatsoever on the part of Research Square concerning the legal status of any country, territory, city or area or of its authorities, or concerning the delimitation of its frontiers or boundaries. This map has been provided by the authors.

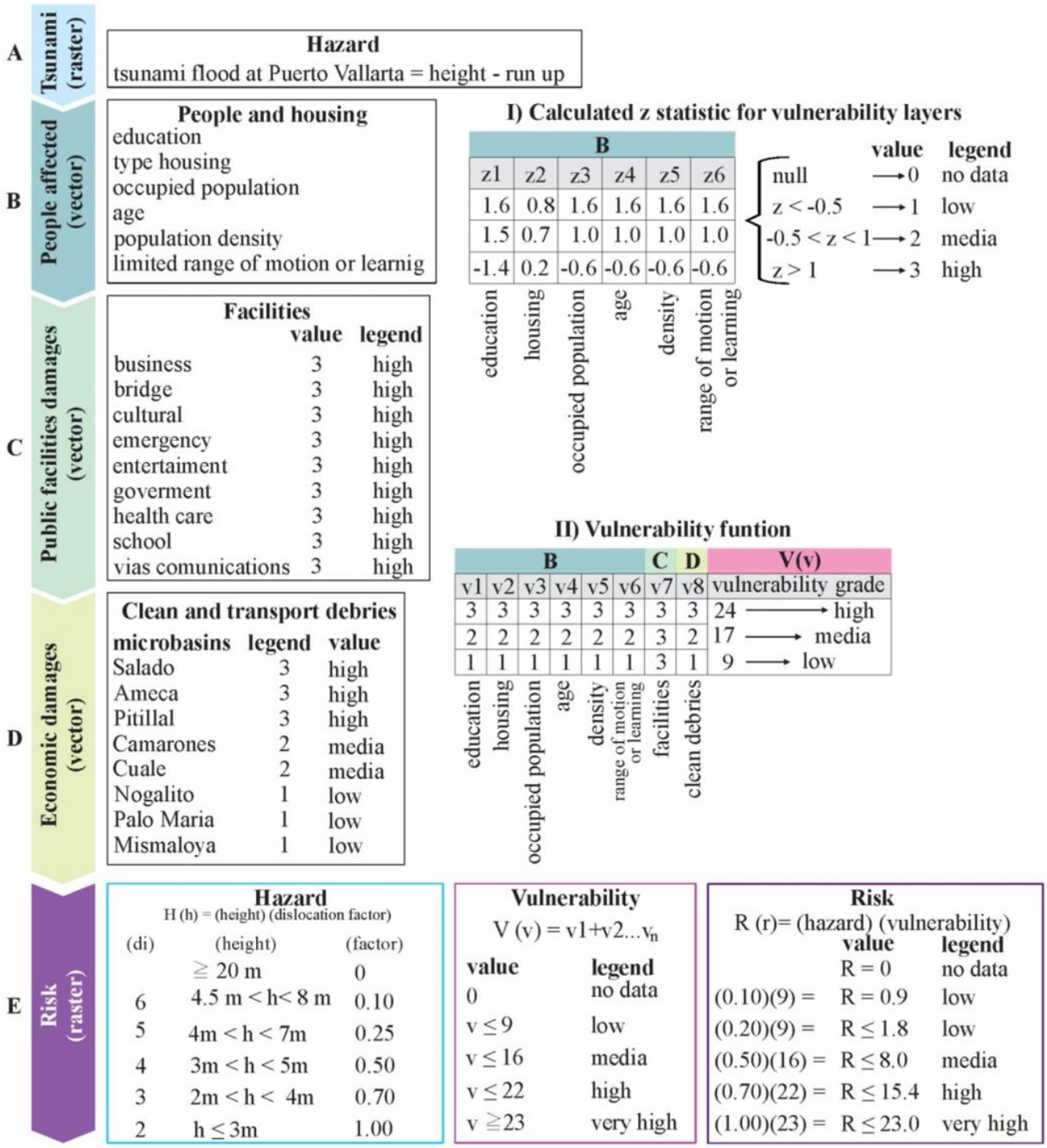

Figure 4

Flowchart to assess vulnerability and risk in the city of Puerto Vallarta.

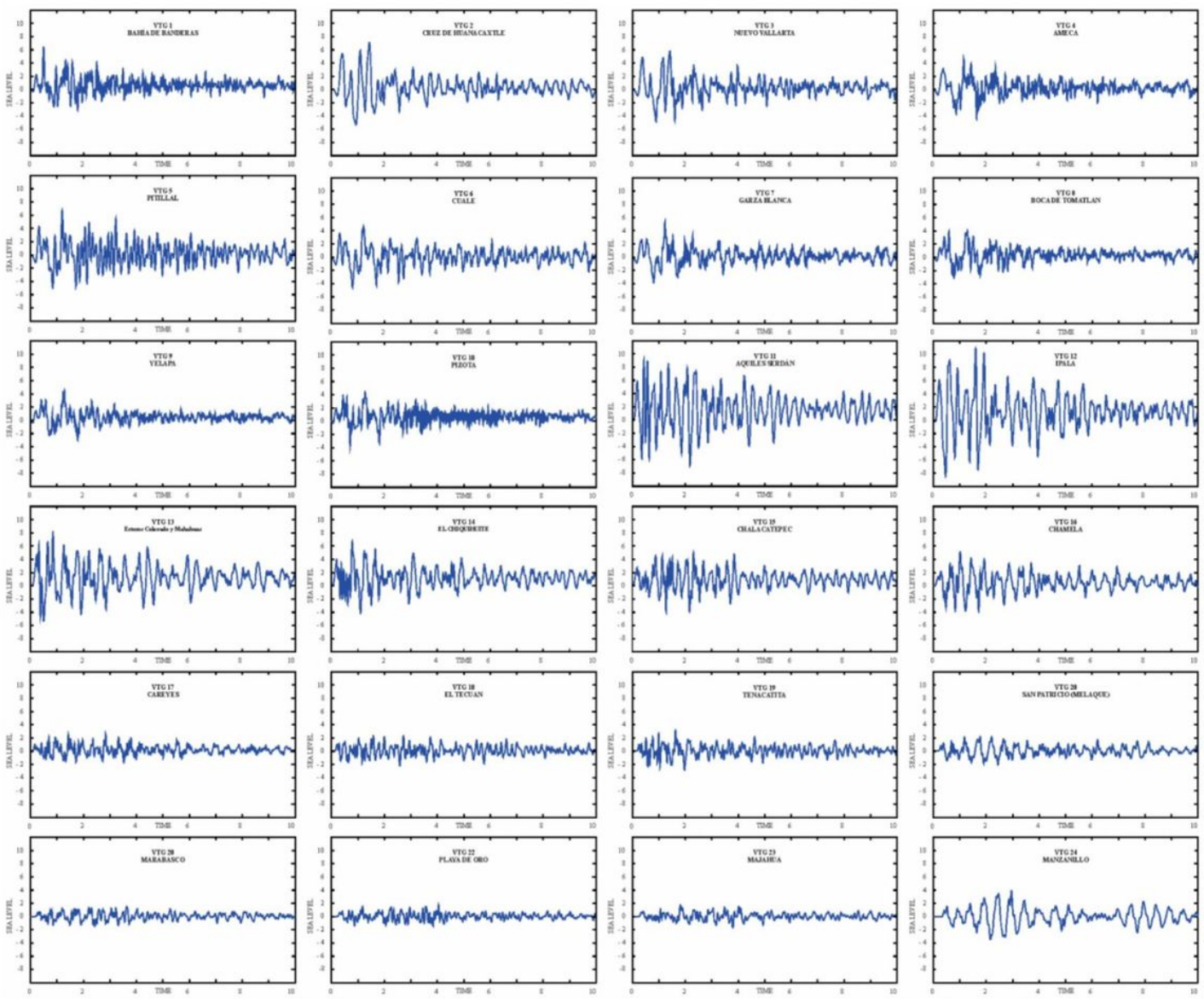

Figure 5

Synthetic tsunami waveforms at obtained the virtual gauge sensors (VTG) in the study region. Sea level in meters, time in hours.

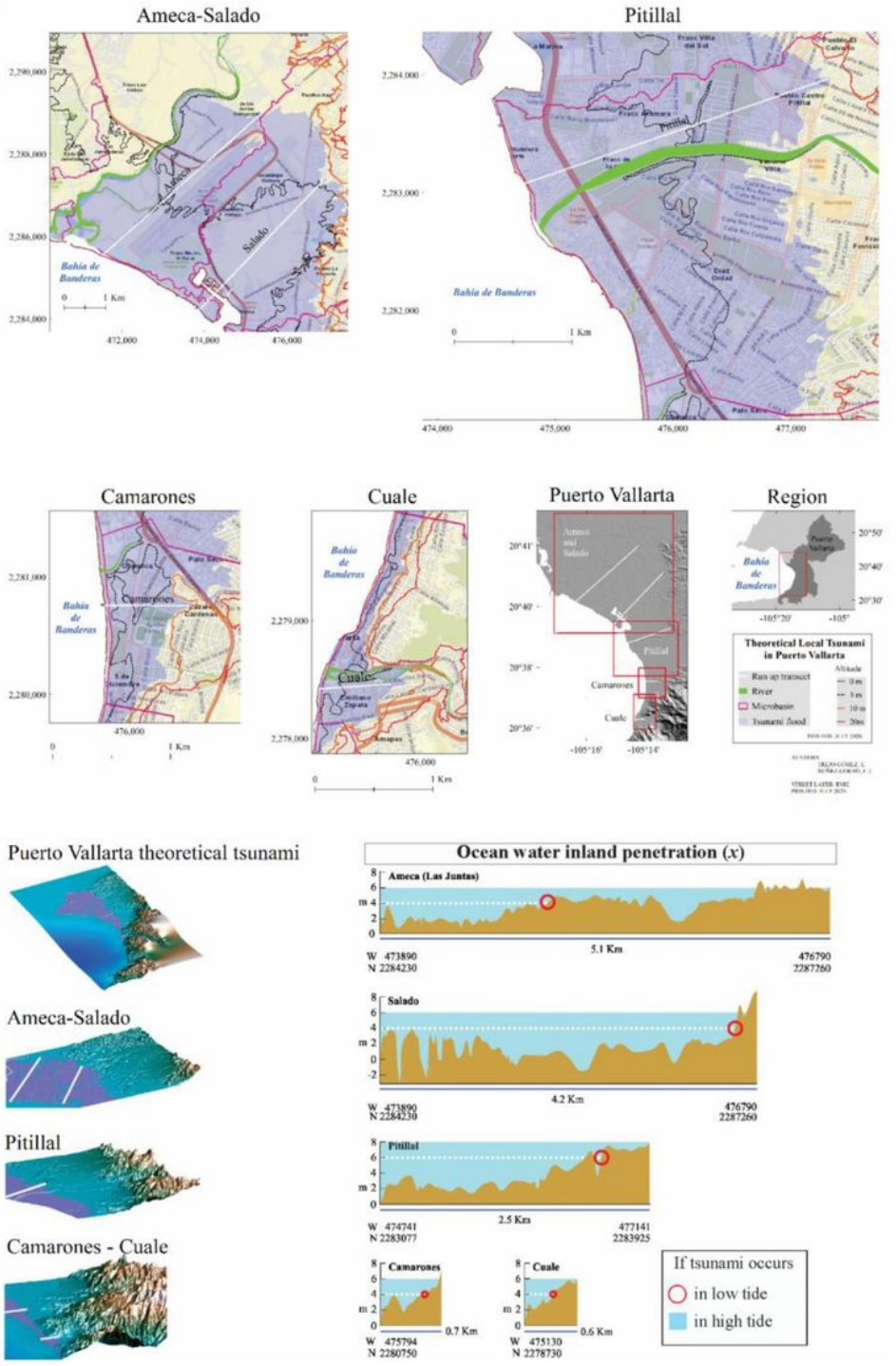

Figure 6

Horizontal inundation distance by a local-tsunami in Puerto Vallarta. Street map by ESRI. Note: The designations employed and the presentation of the material on this map do not imply the expression of any opinion whatsoever on the part of Research Square concerning the legal status of any country, territory, city or area or of its authorities, or concerning the delimitation of its frontiers or boundaries. This map has been provided by the authors.

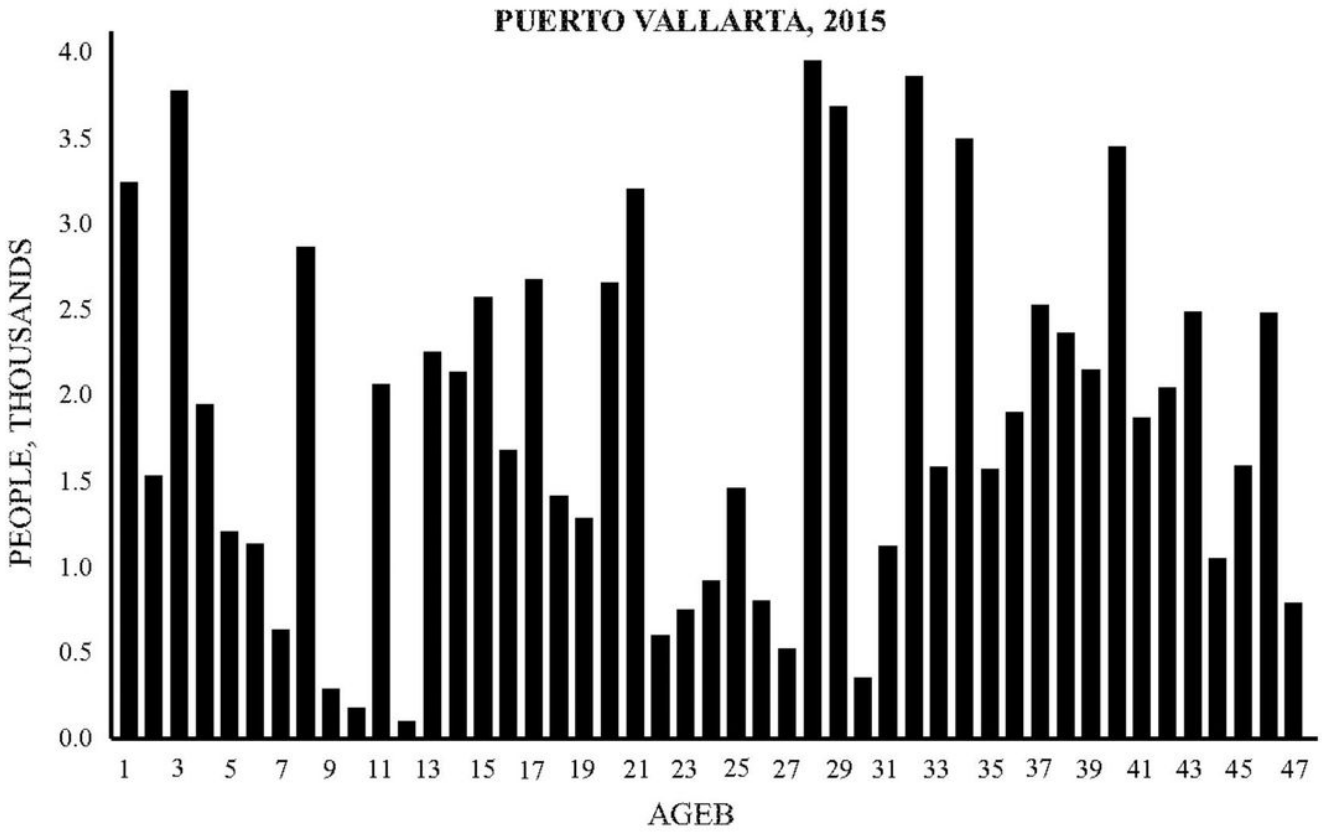

Figure 7

Projection of the affected population in the area of flooding by AGEB.

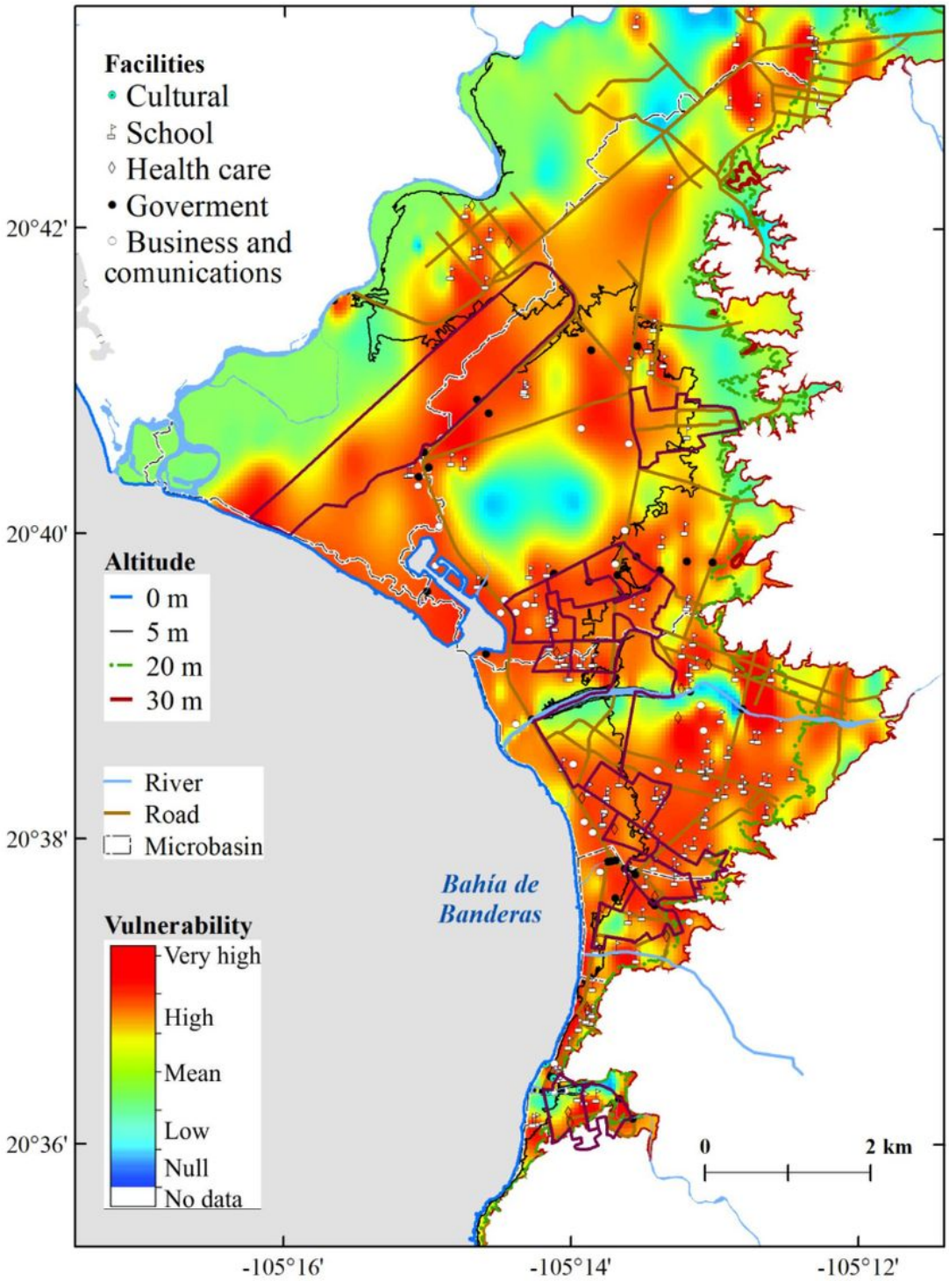

Figure 8

Vulnerability assessment in the municipality of Puerto Vallarta with data from 2015. Note: The designations employed and the presentation of the material on this map do not imply the expression of any opinion whatsoever on the part of Research Square concerning the legal status of any country, territory, city or area or of its authorities, or concerning the delimitation of its frontiers or boundaries. This map has been provided by the authors.

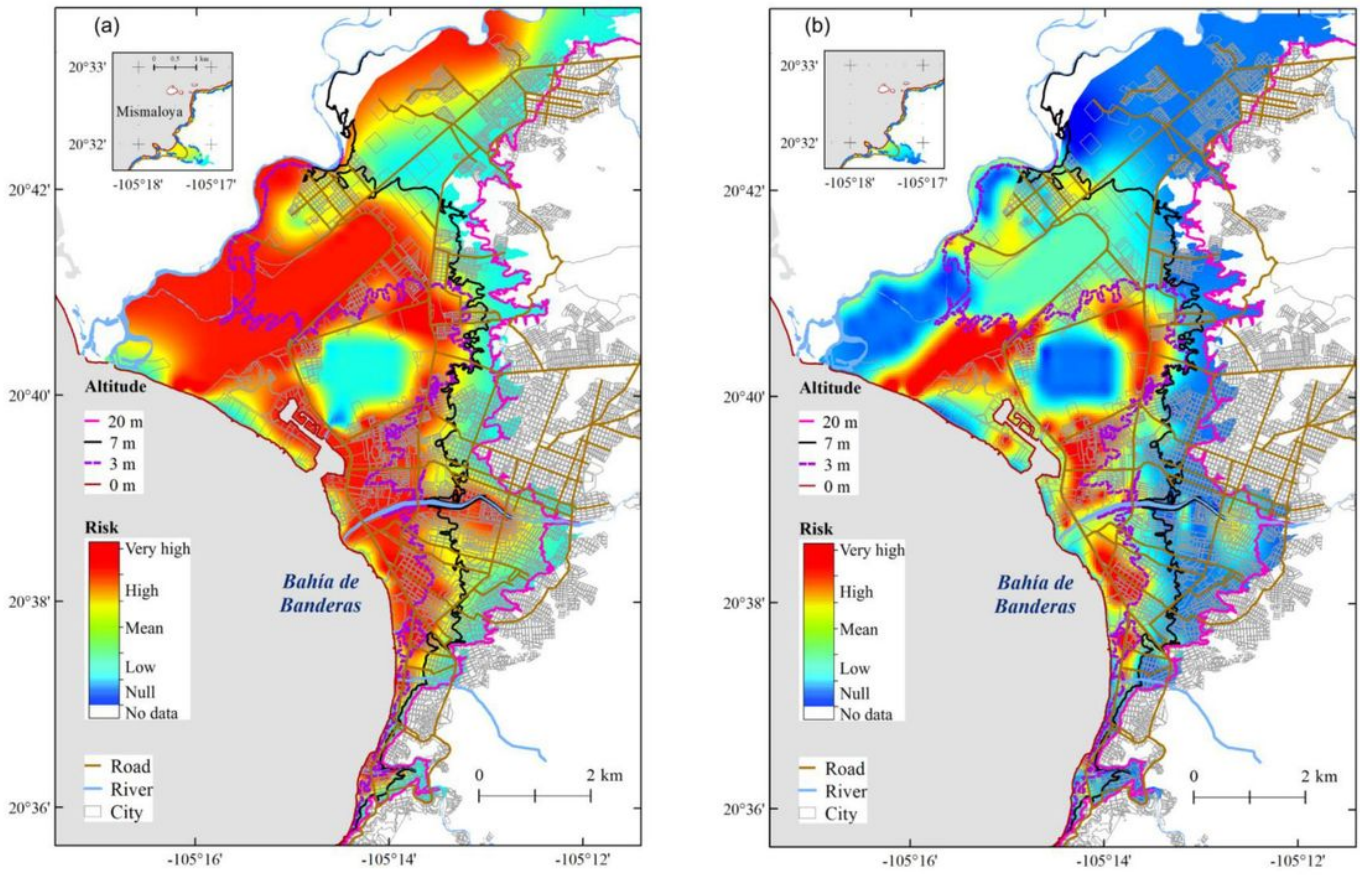

Figure 9

Local-tsunami risk assessment in the municipality of Puerto Vallarta with data from 2015. (a) Total flood area due to a coseismic slip=5m, (b) Risk considering an empiric probability factor due to different values for coseismic slip (Fig. 4). Note: The designations employed and the presentation of the material on this map do not imply the expression of any opinion whatsoever on the part of Research Square concerning the legal status of any country, territory, city or area or of its authorities, or concerning the delimitation of its frontiers or boundaries. This map has been provided by the authors.